Evaporative Cooling & Thermalization of bosonic cold quantum gases

Tara Butler

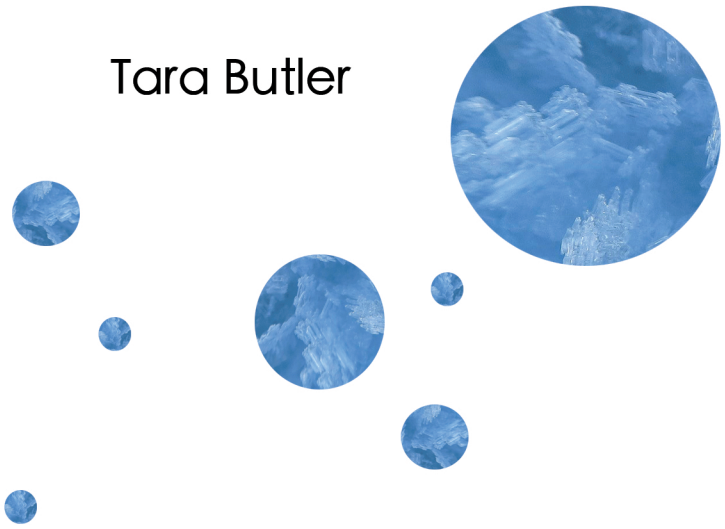

Seminar: Statistical Physics (SS 2020)

Lecturer: Prof. Dr. Georg Wolschin

July 10, 2020

Abstract

The aim of this report is to investigate the possibilities of the evaporative cooling process. Evaporative cooling can be used to cool atoms in a trap to produce a Bose-Einstein condensate. Three different working groups and their results are presented. The Amsterdam model uses kinetic theory to explain the evaporative cooling process, which includes a numerical solution of the Boltzmann equation and points out its effects on the thermodynamic properties of a system. It transpires that the energy distribution can be closely approximated by a truncated Boltzmann distribution. Furthermore, it is shown that it is possible to create a Bose-Einstein condensate with the use of magnetically trapped atomic hydrogen. This model is used by the MIT group for application to their model that includes alkali atoms, and concerns the efficiency of evaporative cooling in different kinds of traps. Finally, the results of the Heidelberg group are presented. Their approach is similar to the kinetic theory used by the Amsterdam group, but concentrates on an analytical solution. Exact analytical solutions of a nonlinear boson diffusion equation are discussed regarding the equilibrium processes that occur in evaporative cooling and thermalization.

Contents

1 Introduction and motivation

What is evaporative cooling?
In general, the term *evaporation* refers to the transition from a liquid to a gaseous state. Highly energetic particles with a finite binding energy can leave a system, which ultimately leads to cooling of the entire system.

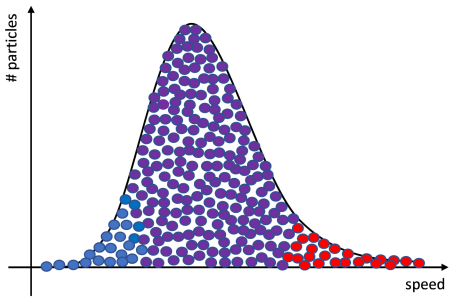

Figure 1: Maxwell-Boltzmann distribution

Evaporative cooling, for example, cools a cup of coffee or may be used for technical water cooling. In addition, evaporating neutrons carry away mega-electron volts of the excitation energies of compound nuclei. In the range of pico−electron volts, the process of evaporative cooling enables sub−microkelvin temperatures to be reached with atoms in a trap. Examples are taken from [10] p. 182.

Why evaporative cooling? What is evaporative cooling good for?
With the help of evaporative cooling, it is possible to lower the temperature of trapped atoms and at the same time increase the phase space density to the extent that Bose-Einstein condensation can be achieved. In addition, its theoretical foundation is based on model-independent considerations, which makes it a highly simple and efficient tool. In 1985 Harald Hess was the first to propose evaporative cooling with the use of trapped atomic hydrogen to produce Bose-Einstein condensates [3].
The first Bose-Einstein condensate was created with rubidium atoms at a temperature of 170nK by Eric Cornell and Karl Wiemann in 1995 [8].
Shortly afterwards, Wolfang Ketterle, a member of the MIT group, also succeeded in producing a Bose-Einstein condensate with sodium atoms.
For producing a Bose-Einstein condensate Cornell, Wiemann and Ketterle received the Nobel Prize in Physics in 2001. Since then, many further experiments with different atom species have been carried out to produce Bose-Einstein condensates in various kinds of traps.

2 Amsterdam Group

This chapter is based on [9] and [11] ch. 3.
The Amsterdam group has developed a model that can be used to describe the evaporative cooling process with kinetic theory. This model makes some assumptions that will be briefly introduced.

2.1 Assumptions and theoretical basis

First, it is assumed that a statistically classical gas is used, i.e. $n\Lambda^3 \ll 1$ with n the atom density and $\Lambda = (2\pi\hbar^2/mkT)^{1/2}$ the thermal de Broglie wavelength.
Secondly, it is assumed that the atoms are trapped in a static potential well. It is then possible for them to escape when their total energy reaches a threshold value, which is chosen to be much higher than their average energy. As a result, the temperature of the gas falls within the trap to reach a new equilibrium value that is established through interatomic collisions.

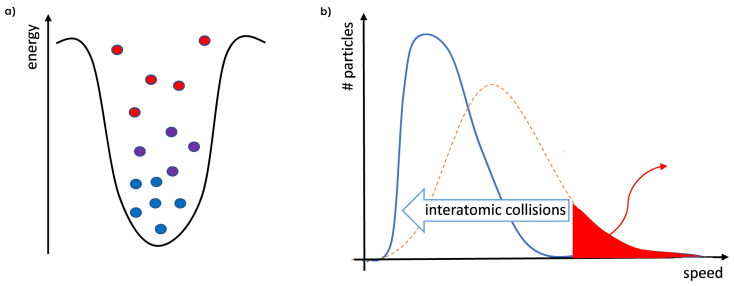

Figure 2: a) Static potential well $U(\mathbf{r})$, b) new equilibrium state at a lower temperature

The basic assumption made by the Amsterdam group is sufficient ergodicity, that is to say, that the distribution of the atoms in phase space depends only on their energy. An example is the ergodic single-particle motion, although many traps have a partly non-ergodic single-particle motion. This is why interatomic collisions are required to guarantee this assumption.
By using these assumptions, all of the necessary details regarding the trapped potential $U(\mathbf{r})$ can be found in the energy density of states:

$$\rho(\epsilon) \equiv (2\pi\hbar)^{-3} \int d\mathbf{r}\; d\mathbf{p}\; \delta(\epsilon - U(\mathbf{r}) - p^2/2m)\;. \tag{2.1}$$

After evaluating the momentum integral, the following results:

$$\rho(\epsilon) = \frac{2\pi(2m)^{3/2}}{(2\pi\hbar)^3} \int_{U(\mathbf{r})\leq\epsilon} d\mathbf{r}\; \sqrt{\epsilon - U(\mathbf{r})} \tag{2.2}$$

which leads to the expression of the power-law density of states:

$$\rho(\epsilon) = A_{PL}\ \epsilon^{1/2+\delta} \tag{2.3}$$

for simple kinds of traps such as harmonic traps with $\delta = \frac{3}{2}$, square traps with $\delta = 0$, spherical-quadrupole traps with $\delta = 3$ and A_{PL} as a trap dependent constant.

2.2 Truncated energy distribution

Evaporative cooling is a non-equilibrium process. However, interatomic collisions lead to a thermal redistribution of energy, which is why the distribution function in a quasi-equilibrium results as follows:

$$f(\epsilon) = \sum_{l=1}^{\infty} z^l\ \exp[-l\epsilon/kT]\ \Theta(\epsilon_t - \epsilon)\ . \tag{2.4}$$

The Heaviside's unit step function Θ represents the atoms cut off from the distribution with $\epsilon > \epsilon_t$. This distribution has three independent parameters: the degeneracy parameter z, the quasi-temperature T, and the truncation energy ϵ_t. For the discussion of evaporative cooling it is sufficient to consider only the first term of the truncated exponential energy distribution of the non-degenerate regime:

$$f(\epsilon) = z\ e^{-\epsilon/kT}\ \Theta(\epsilon_t - \epsilon) \tag{2.5}$$

with the normalization condition for the total number N of trapped atoms:

$$N = z\int_0^{\epsilon_t} d\epsilon\ \rho(\epsilon)\ e^{-\epsilon/kT}\ . \tag{2.6}$$

2.3 Thermodynamic properties

This chapter will now illustrate how the thermal properties of a system change due to the truncation edge.

2.3.1 Canonical partition function

By rewriting equation (2.6) to

$$N = \underbrace{n_0\Lambda^3}_{\equiv\ z}\zeta \tag{2.7}$$

with

$$\zeta = \int_0^{\epsilon_t} d\epsilon\ \rho(\epsilon)\ e^{-\epsilon/kT} \tag{2.8}$$

and using equation (2.1) together with the definition of the classical single particle Hamiltonian $H(\mathbf{r},\mathbf{p}) = U(\mathbf{r}) + p^2/2m$, the expression for the classical canonical partition function results:

$$\zeta = (2\pi\hbar)^{-3} \int d\mathbf{p}\; d\mathbf{r}\; e^{-H(\mathbf{r},\mathbf{p})/kT}\; \Theta[\epsilon_t - H(\mathbf{r},\mathbf{p})]\;. \tag{2.9}$$

As before, the Heaviside's unit step function Θ represents the atoms cut off from the distribution with $U(\mathbf{r}) + p^2/2m \geq \epsilon_t$.

2.3.2 Density distribution

The expression for the density distribution $n(\mathbf{r})$ results from the calculation of the momentum integral of the partition function given in (2.7):

$$n(\mathbf{r}) = \underbrace{n_0\; e^{-U(\mathbf{r})/kT}}_{=\; n_\infty(\mathbf{r})} P\Big(\frac{3}{2}, \eta_t(\mathbf{r})\Big) \tag{2.10}$$

with the incomplete gamma function $P(a,\eta)$ (see appendix 6.2) and $\eta_t(\mathbf{r}) \equiv (\epsilon_t - U(\mathbf{r})/kT$. Figure 3 shows the density distribution and its change with respect to the truncation in phase space.

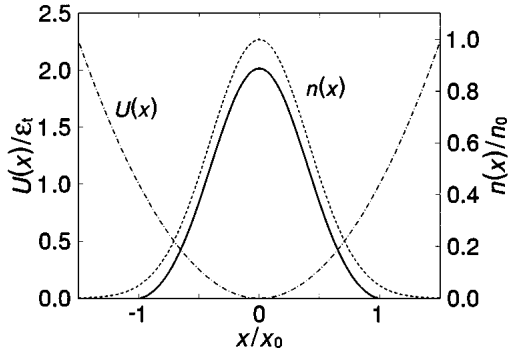

Figure 3: Density distribution: $n_\infty(x)$ (dashed), $n(x) = n_\infty(x)P(3/2, \eta_t(x))$, potential $U(x)$ (dot-dashed) with $U(x_0) = \epsilon_t$, [9].

2.3.3 Reference volume

The introduction of a reference volume V_e also often proves to be very useful:

$$V_e = N/n_0 \tag{2.11}$$

with the total number of trapped atoms N and the reference density n_0.
To obtain a simple temperature dependency with regard to the reference volume for deep power-law traps, it makes sense to first rewrite the expression of the partition function

using the power law density of states (2.3):

$$\zeta = A_{PL} \int_0^{\epsilon_t} d\epsilon \; \epsilon^{1/2+\delta} \; e^{-\epsilon/kT} = \zeta_\infty P\Big(\frac{3}{2} + \delta, \eta\Big) \tag{2.12}$$

with the expression for infinitely deep traps $\zeta_\infty = A_{PL}[kT]^{3/2+\delta} \; \Gamma\Big(\frac{3}{2} + \delta\Big)$ and the Euler gamma function Γ.
The following results for the reference volume:

$$V_e = \Lambda^3 \zeta_\infty P\Big(\frac{3}{2} + \delta, \eta\Big) \tag{2.13}$$

which leads to an interesting fact of deep power-law traps:

$$V_e \propto T^\delta \quad \text{for} \quad \eta \to \infty \; . \tag{2.14}$$

2.3.4 Internal energy

The expression for the internal energy E, which is composed of the energy density of states $\rho(\epsilon)$ and the distribution function $f(\epsilon)$, results in an expression known from statistical mechanics, using the expression for the partition function:

$$E = \int d\epsilon \; \rho(\epsilon) f(\epsilon) = NkT^2 \frac{1}{\zeta} \frac{\partial \zeta}{\partial T} \; . \tag{2.15}$$

By using $\zeta = V_e \Lambda^3$, it follows that:

$$E = \Big(\frac{3}{2} + \tilde{\gamma}\Big) NkT \tag{2.16}$$

with the scaling parameter $\tilde{\gamma}$

$$\tilde{\gamma} = \Big(\frac{\partial \ln V_e}{\partial \ln T}\Big)_{\epsilon_t} \; . \tag{2.17}$$

From equations (2.15) and (2.8) it can be seen that the internal energy depends only on two independent variables N and T, since in this model the truncation energy ϵ_t is kept constant. Hence it follows that:

$$dE = C_{\epsilon_t} dT + \mu_{\epsilon_t} dN \tag{2.18}$$

with the heat capacity

$$C_{\epsilon_t} = \Big(\frac{3}{2} + \tilde{\gamma} + T(\partial\tilde{\gamma}/\partial T)_{\epsilon_t}\Big) Nk \tag{2.19}$$

and the chemical potential

$$\mu_{\epsilon_t} = \Big(\frac{3}{2} + \tilde{\gamma}\Big) kT \ . \tag{2.20}$$

This means that the expression for μ_{ϵ_t} is composed of the average energy per trapped atoms: $\mu = E/N$.

2.4 Kinetic equation

Taking into account sufficient ergodicity, the Boltzmann equation can be reduced to the following kinetic equation for the distribution function $f(\epsilon)$ of a classical gas [9]:

$$\rho(\epsilon_4)\dot{f}(\epsilon_4) = \frac{m\sigma}{\pi^2\hbar^3} \int d\epsilon_1 d\epsilon_2 d\epsilon_3 \ \delta(\epsilon_1 + \epsilon_2 - \epsilon_3 - \epsilon_4) \ \rho(\min[\epsilon_1, \epsilon_2, \epsilon_3, \epsilon_4])\{f(\epsilon_1)f(\epsilon_2) - f(\epsilon_3)f\epsilon_4)\} \tag{2.21}$$

with an energy-independent cross section $\sigma = 8\pi a^2$, where a is the scattering length. This equation characterizes the time evolution of the energy distribution function $f(\epsilon)$ due to the collisions between atoms.

2.4.1 Numerical solution

The integration of the kinetic equation can be performed numerically using a Euler method. Figure 4 shows the evolution of the distribution function at different times by comparing the calculated distribution to the best-fit Boltzmann form, with the inset displaying the energy distribution. The total number of collisions per atom is shown on the right axis. Clearly, the calculated distribution fits very well by a simple exponential at all times.

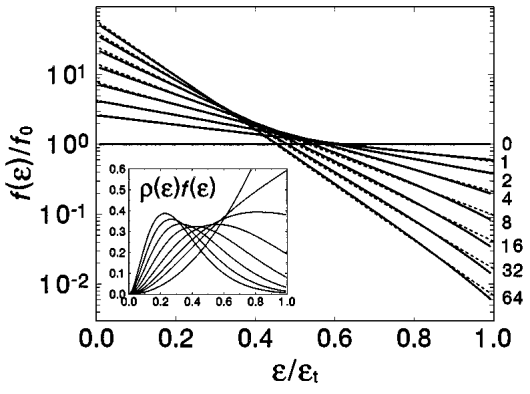

Figure 4: Evolution of the distribution function $f(\epsilon)$: calculated distribution (solid), best-fit Boltzmann form (dashed), inset: energy distribution $\rho(\epsilon)f(\epsilon)$, [9].

2.4.2 Evaporation rate

The expression for the evaporation rate in the truncated Boltzmann approximation represents the loss rate of atoms to non-trapped states. This means that the kinetic equation is integrated using the truncated Boltzmann distribution over the untrapped energy states, which leads to the following expression:

$$\dot{N}_{ev} = -\int_{\epsilon_t}^{\infty} d\epsilon_4 \; \rho(\epsilon_4) \; \dot{f}(\epsilon_4) \; . \tag{2.22}$$

By using that $\epsilon_4 > \epsilon_t > \epsilon_1, \epsilon_2$ and $\epsilon_3 = \epsilon_1 + \epsilon_2 - \epsilon_4$, equation (2.22) can be written as follows:

$$\dot{N}_{ev} = -\frac{m\sigma}{\pi^2\hbar^3} \int_0^{\epsilon_t} d\epsilon_3 \int_{\epsilon_3}^{\epsilon_t} d\epsilon_2 \int_{\epsilon_3+\epsilon_t-\epsilon_2}^{\epsilon_t} d\epsilon_1 \; \rho(\epsilon_3) \; f(\epsilon_1) \; f(\epsilon_2) \tag{2.23}$$

so that the following expression for the evaporation rate results:

$$\dot{N}_{ev} = -n_0^2 \bar{v} \sigma e^{-\eta} V_{ev} \tag{2.24}$$

with the mean thermal speed $\bar{v} \equiv [8kT/\pi m]^{1/2}$ and the reference volume as

$$V_{ev} = \frac{\Lambda^3}{kT} \int_0^{\epsilon_t} d\epsilon \; \rho(\epsilon)[(\epsilon_t - \epsilon - kT)e^{-\epsilon/kT} + kTe^{-\epsilon_t/kT}] \; . \tag{2.25}$$

2.4.3 Loss of internal energy

The loss of internal energy that arises during the evaporative cooling process is composed of two different components:

$$\dot{E} = \dot{E}_{ev} + \dot{E}_t \; . \tag{2.26}$$

The first term − the evaporation term − characterizes the loss of energy resulting from the atoms eliminated during the evaporative cooling process:

$$\dot{E}_{ev} = -\int_{\epsilon_t}^{\infty} d\epsilon_4 \; \epsilon_4 \; \rho(\epsilon_4) \dot{f}(\epsilon_4) \; . \tag{2.27}$$

The second term − the truncation term − results in a changed truncation energy, i.e. a lowering of the threshold value during the evaporative cooling process:

$$\dot{E}_t = \epsilon_t \rho(\epsilon_t) f(\epsilon_t) \dot{\epsilon}_t = \epsilon_t \dot{N}_t \; . \tag{2.28}$$

However, the second term plays no role in this model, since the truncation parameter ϵ_t is assumed to be constant.

For the evaporation term the following expression results:

$$\dot{E}_{ev} = \dot{N}_{ev}[\epsilon_t + (1 - X_{ev}/V_{ev})kT] \tag{2.29}$$

with

$$X_{ev} = \frac{\Lambda^3}{kT} \int_0^{\epsilon_t} d\epsilon \; \rho(\epsilon)[kTe^{-\epsilon/kT} - (\epsilon_t - \epsilon + kT)e^{-\epsilon_t/kT}] \; . \tag{2.30}$$

This equation represents the amount of internal energy lost by the removed atoms, which is slightly larger than the energy of the truncation edge ϵ_t.

2.4.4 Comparison of results

The aim of this section is to compare and discuss the assumptions presented in the preceding sections of a truncated Boltzmann approximation and the integration of the kinetic equation.
With the previously derived expression for the evolution of the state

$$\dot{E} = C\dot{T} + \mu\dot{N} \tag{2.31}$$

one first obtains two differential equations for the temperature T and the number of trapped atoms N:

$$\dot{T} = \frac{\dot{E}_{ev} - \mu\dot{N}_{ev}}{C} \tag{2.32}$$

and

$$\dot{N} = \dot{N}_{ev} \tag{2.33}$$

where the constant truncation energy from equation (2.31) was used again. This means that there is no additional truncation loss rate to consider.
The curves in Figure 5 present the results obtained by integrating the two differential equations with respect to the truncated Boltzmann approximation. The symbols were created following the numerical integration of the kinetic equation by fitting an exponential to the energy distribution.
The curves match the symbols very accurately. Accordingly, the assumption of a truncated Boltzmann distribution and its approximation are applicable for the energy distribution.

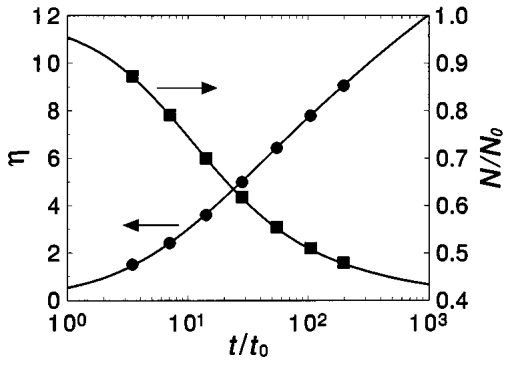

Figure 5: Truncation parameter η (circles) and the fraction of atoms remaining in trap N/N_0 (squares) as a function of time t/t_0, [9].

2.5 Cooling atomic hydrogen

This section discusses the evaporative cooling process based on magnetically trapped atomic hydrogen, followed by its application for realizing Bose-Einstein condensates.

2.5.1 Relaxation and heating

In the Amsterdam group model, magnetically trapped atomic hydrogen is used for the discussion of the evaporative cooling process. However, magnetic relaxation, which primarily removes low-energy atoms, leads to heating. It is assumed here that atoms in both trapped and untrapped spin states produced by relaxation events can leave the gas.
Regarding the rate of change of the number of trapped atoms due to spin relaxation, the following results:

$$\dot{N}_{rel} = -n_0^2 G V_{2e} \tag{2.34}$$

with a temperature-independent rate constant G and the effective volume for binary collisions:

$$V_{2e}(T) = \int d^3r \; [n(\mathbf{r})/n_0]^2 \; . \tag{2.35}$$

For the rate of change of the internal energy one obtains:

$$\dot{E}_{rel} = \dot{N}_{rel}\Big(\frac{3}{2} + \tilde{\gamma_2}\Big)kT \tag{2.36}$$

with the scaling parameter $\tilde{\gamma_2}(T) = [T/(2V_{2e})]\partial V_{2e}/\partial T$.

2.5.2 Thermalization ratio

Due to the fact that evaporation and relaxation have the same density dependency, there are two combined expressions for both the energy loss rate and the atomic loss rate:

$$\dot{E}_{ev} + \dot{E}_{rel} = \dot{N}_{ev}[\eta + (1 - X_{ev}/V_{ev}) + (3/2 + \tilde{\gamma_2})/R]kT \tag{2.37}$$

with the thermalization ratio

$$R = \dot{N}_{ev}/\dot{N}_{rel} = \frac{\bar{v}\sigma}{G}\frac{V_{ev}}{V_{2e}}e^{-\eta} \tag{2.38}$$

and

$$\dot{N}_{ev} + \dot{N}_{rel} = \dot{N}_{ev}[1 + 1/R] \ . \tag{2.39}$$

The thermalization ratio R decreases with decreasing temperature ($R \propto T^{1/2}$), so it is useful to introduce a characteristic temperature T_* at which the probability of an elastic or inelastic collision for an atom is equal:

$$kT_* = \frac{\pi m G^2}{16\sigma^2} \ . \tag{2.40}$$

2.5.3 Bose-Einstein condensation with atomic hydrogen

The characteristic temperature for atomic hydrogen is $T_* = 1.4$ nK with the rate constant $G = 10^{-15}\mathrm{cm}^3\mathrm{s}^{-1}$ and scattering length $a = 0.072$.
Figure 6 shows three characteristic temperatures of atomic hydrogen. Curve a) shows the minimum temperature reached in the long-time limit. Curve b) shows the temperature at which the maximum phase space density $n_0\Lambda^3$ is reached. Curve c) shows the temperature at which the maximum reference density n_0 is reached.
With increasing reference density n_0, cooling only works for $T > 2$ μK. However, for increasing phase space density $n_0\Lambda^3$ it is possible to cool to $T = 25$ nK.
This result indicates that with the help of magnetically trapped atomic hydrogen it is possible to achieve a temperature with increasing phase space density that is sufficiently low to obtain Bose-Einstein condensates.

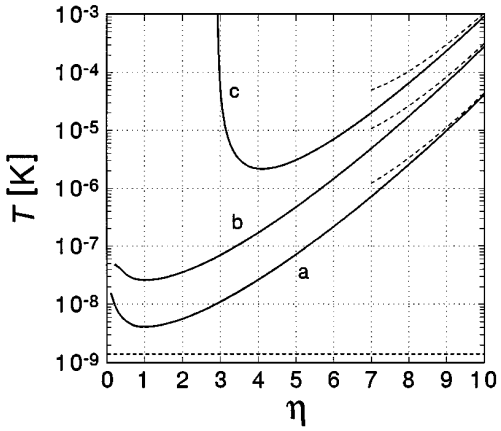

Figure 6: Characteristic temperatures of atomic hydrogen in a harmonic trap as a function of η: a) asymptotic temperature, b) lowest temperature with increasing phase space density $n_0\Lambda^3$, c) lowest temperature with increasing reference density n_0. Dashed lines: curves without corrections due to truncation; horizontal dashed lines: scale temperature T_*, [9].

3 MIT Group

The following chapter is based on [10] ch. 2.
The MIT group has developed a model with the use of analytical expressions to describe and discuss the dynamics of the evaporative cooling process with alkali atoms. This chapter demonstrates how the Amsterdam model can be applied to this situation in order to analyze the efficiency of different types of traps.

3.1 Scaling behavior

The important quantities for the evaporative cooling process can be represented by logarithmic derivatives:

$$\alpha = \frac{d(\ln T)}{d(\ln N)} = \frac{\dot{T}/T}{\dot{N}/N} \ . \tag{3.1}$$

The parameter α represents the temperature decrease per particle loss. An expression for the relationship between the average energy of escaping atoms and α can thus be formulated:

$$\alpha = \frac{\eta + \kappa}{\delta + 3/2} - 1 \tag{3.2}$$

with a small number κ defined by $\kappa = 1 - X_{ev}/V_{ev}$ as derived in section 2.4.3. Physically, this equation expresses how much more than the average energy is removed by an atom, [10] p. 186.

3.2 Runaway evaporation

In the case of alkali atoms with a dominant loss mechanism due to background gas collisions, a constant or increasing elastic collision rate $n\sigma v$ is of great importance for the evaporative cooling process. This is called *runaway evaporation*.
Taking into account the scale behavior for the elastic collision rate $n\sigma v$ (see appendix 6.2), the expression for the variation of the elastic collision rate holds:

$$\frac{d(n\sigma v)}{dt}\Big/ n\sigma v = \frac{1}{\tau_{el}}\Big(\frac{\alpha(\delta - 1/2) - 1}{\lambda} - \frac{1}{R}\Big) \tag{3.3}$$

with the cross section σ, the number of elastic collisions per trapping time R and the ratio between the time constant for evaporation τ_{el} and the elastic collision time τ_{el}: $\lambda = \tau_{ev}/\tau_{el}$, where $1/\tau_{el} = n_0\sigma\bar{v}\sqrt{2}$. In the limit for large η the following applies:

$$\lambda = \frac{\sqrt{2}e^{\eta}}{\eta} \ . \tag{3.4}$$

The requirement for runaway evaporation is:

$$R \geq R_{min} = \frac{\lambda}{\alpha(\delta - 1/2) - 1} \ . \tag{3.5}$$

Figure 7 shows the minimum number of elastic collisions per trapping time for parabolic and linear potentials. The results of the Amsterdam group were used for the parabolic (solid) and the linear (dashed) potential, whereas for the parabolic potential (dash-dotted) the expressions for α (3.2) and λ (3.4) were used. Evidently, the linear potential has an R_{min} ratio three to four times smaller compared to the parabolic potential.

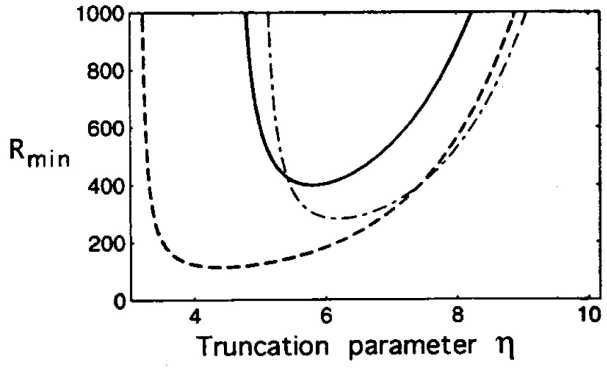

Figure 7: The minimum ratio R_{min} as a function of the truncation parameter η, parabolic potentials (solid and dash-dotted), and linear potential (dashed) [10].

The phase space density increase with time can be expressed by (see appendix 6.2):

$$\beta = 100\tau_{el}\frac{d}{dt}(\log_{10}D) = \frac{100}{\ln 10}\Big(\frac{\alpha(\delta+3/2)-1}{\lambda} - \frac{1}{R}\Big) \ . \tag{3.6}$$

Figure 8 shows the increase in phase space density D for different values of R. In the range of small R and large η, β becomes negative. This is because a slow evaporative cooling process cannot balance out the losses caused by background gas collisions.

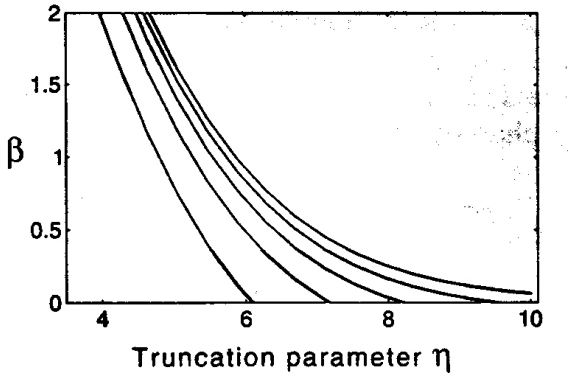

Figure 8: Increase of phase space density β per 100 elastic collision times as a function of the truncation parameter η. Evolution of R: infinite (upper line), 500, 200, 100, 50 (lower line), [10].

3.3 Comparison between alkali atoms and atomic hydrogen

This section discusses and compares the differences and possibilities of evaporative cooling with alkali atoms and atomic hydrogen.
The relative increase in phase space density with decreasing number N can be expressed by:

$$\gamma = -\frac{d(\ln D)}{d(\ln N)} = \frac{\alpha(\delta+3/2)}{1+\lambda/R} - 1 \ . \tag{3.7}$$

As mentioned, evaporative cooling is used to lower the temperature while increasing the phase space density. However, in order to obtain Bose-Einstein condensates with a large number of atoms, the aim is to carry out this process with the smallest possible loss in the number of atoms. This aim is achieved with the largest possible γ, so this parameter is also referred to as the *efficiency parameter*.
In the case of alkali atoms with a dominant loss mechanism due to background gas collisions, this situation can be explained using the following expression:

$$-\frac{d(\ln R)}{d(\ln N)} = \frac{\alpha(\delta-1/2)}{1+\lambda/R} - 1 \ . \tag{3.8}$$

R varies exponentially with $1/N$, which means that with a negative exponent, R also decreases. Therefore, the efficiency parameter γ decreases and becomes zero, so that no increase in the phase space density is possible. For this reason, an attempt is made to begin with the largest possible R to ensure an increase during the evaporative cooling process. However, when the runaway evaporation threshold is reached, R remains constant or increases, which in turn means that the efficiency is only affected by other loss mechanisms, such as three-body recombination or dipolar relaxation.
In the case of atomic hydrogen, all experiments were carried out in a cryogenic environment in which background gas collisions were negligible. Here, the dominant loss mechanism is inelastic binary collision, such that during the evaporative cooling process no increase in R and therefore no increase in efficiency is possible. Accordingly, the maximum increase in phase space density could only be obtained with a small efficiency parameter γ.

4 Heidelberg Group

The following chapter is based on [15] and [16].
The Heidelberg group presents an exact analytical solution of a nonlinear boson diffusion equation with initial conditions that characterize the evaporative cooling process. This chapter demonstrates that considering a singularity with boundary conditions is essential for obtaining physically relevant solutions.

4.1 Free solutions

The expression for the transport equation for the single-particle occupation probability distributions $n \equiv n_{th}(\epsilon, t)$ results from the bosonic Boltzmann collision term [13]:

$$\frac{\partial n}{\partial t} = -\frac{\partial}{\partial \epsilon}\Big[vn(1+n) + n\frac{\partial D}{\partial \epsilon}\Big] + \frac{\partial^2}{\partial \epsilon^2}[Dn] \tag{4.1}$$

with the drift term $v(\epsilon, t)$ and the diffusion term $D(\epsilon, t)$. In the limit of energy-independent transport coefficients D and v it applies:

$$\frac{\partial n}{\partial t} = -v\frac{\partial}{\partial \epsilon}\Big[n(1+n)\Big] + D\frac{\partial^2 n}{\partial \epsilon^2}\ . \tag{4.2}$$

The thermal equilibrium distribution can be expressed by a stationary solution:

$$n_{eq}(\epsilon) = \frac{1}{e^{(\epsilon-\mu)/T} - 1} \tag{4.3}$$

with $T = -D/v$ and the chemical potential $\mu < 0$. The nonlinear boson diffusion equation (NBDE) with a given initial condition can now be solved exactly using a nonlinear

transformation [14]:

$$n(\epsilon,t) = -\frac{D}{v}\frac{\partial}{\partial\epsilon}\ln Z(\epsilon,t) - \frac{1}{2} = -\frac{D}{v}\frac{1}{Z}\frac{\partial Z}{\partial\epsilon} - \frac{1}{2} \tag{4.4}$$

where the time-dependent partition function $Z(\epsilon,t)$ follows a linear diffusion equation:

$$\frac{\partial}{\partial t}Z(\epsilon,t) = D\frac{\partial^2}{\partial\epsilon^2}Z(\epsilon,t)\ . \tag{4.5}$$

In the case of a free partition function without boundary conditions, the following expression applies:

$$Z_{free}(\epsilon,t) = a(t)\int_{-\infty}^{+\infty} G_{free}(\epsilon,x,t)F(x)dx \tag{4.6}$$

with an energy-independent prefactor $a(t)$, and the free Green's function $G_{free}(\epsilon,x,t)$ represented by a Gaussian:

$$G_{free}(\epsilon,x,t) = \exp\Big(-\frac{(\epsilon-x)^2}{4Dt}\Big) \tag{4.7}$$

and the function $F(x)$:

$$F(x) = \exp\Big[-\frac{1}{2D}(vx + 2v\underbrace{\int_0^x n_i(y)dy)}_{=A_i(x)}\Big]\ . \tag{4.8}$$

The definite integral with occupation number distribution n_i can be replaced by an indefinite expression $A_i(x)$ over the initial distribution, because at the lower limit it is eliminated in the calculation of $n(\epsilon,t)$ due to the logarithmic derivative. With this replacement, a singularity can be included at negative energies in the integral. Since there is no physical interpretation for negative energies below the singularity at the chemical potential, the focus lies on the positive energy region.
When calculating solutions with regard to the singularity at $x = \mu$, however, a shift arises in the chemical potential:

$$\mu' = \frac{D}{v}\ln\Big[z^{-1} - \exp(-\epsilon_i/T)\Big]\ . \tag{4.9}$$

This is caused by the choice of the free Green's function $G_{free}(\epsilon,x,t)$, but the expression reveals that the chemical potential μ is no longer restricted to negative values, as should be the case in a system with bosons. Furthermore, this shift violates the conservation of the number of particles. For this reason, a boundary condition $n(\epsilon=\mu,t)=\infty$ is placed at the singularity $\epsilon=\mu$ by considering the chemical potential as a fixed parameter.

4.2 Exact solutions with boundary conditions

By introducing the chemical potential as a fixed parameter the NBDE must be solved with one static zero point in the partition function: $\lim_{\epsilon\to\mu} n(\epsilon,t) = \infty \ \forall \ t$ so that $Z(\mu,t) = 0$. This produces a new Green's function that vanishes at $\epsilon = \mu \ \forall \ t$:

$$G(\epsilon,x,t) = G_{free}(\epsilon-\mu,x,t) - G_{free}(\epsilon-\mu,-x,t) \tag{4.10}$$

with the associated partition function:

$$Z(\epsilon,t) = \int_0^\infty G(\epsilon,x,t)\ F(x+\mu)\ dx \tag{4.11}$$

whereby the energy region is restricted to $\epsilon \geq \mu$ due to the new Green's function.
To be able to discuss the evaporative cooling process, a truncated thermal equilibrium distribution can be selected as the initial condition, with a cutoff at which atoms with high energies are eliminated:

$$n_i(\epsilon) = \frac{1}{e^{(\epsilon-\mu)/T}-1}\Theta(1-\epsilon/\epsilon_i)\ . \tag{4.12}$$

Two different cases can now be distinguished. The first case is described by identical initial and final temperatures. In such a situation no cooling process takes place. The second case is described by an initial temperature that differs from the final temperature, so that a cooling process can take place.

4.2.1 $T_i = T_f$

The solution at a constant temperature T can be represented by the following expression, similar to a Bose-Einstein distribution:

$$n(\epsilon,t) = \frac{1}{exp\Big(\frac{\epsilon-\mu}{T}\Big)L(\epsilon,t)-1} \tag{4.13}$$

with the function $L(\epsilon,t)$, which describes the time evolution towards the equilibrium distribution. Figure 9 shows the equilibration with respect to the NBDE. Clearly, the cutoff at $\epsilon_i = 7$peV is smeared out for short times, while at large times of $t = 40$ms the solution returns to the initial equilibrium at temperature T, as the temperature is kept constant in this situation.

4.2.2 $T_i \neq T_f$

The case with an initial temperature T_i that differs from the final temperature T_f can first be described using a linear relaxation ansatz $\partial n_{rel}/\partial t = (n_{eq} - n_{rel})/\tau_{eq}$ with

$$n_{rel}(\epsilon,t) = n_i(\epsilon)e^{-t/\tau_{eq}} + n_{eq}(\epsilon)(1-e^{-t/\tau_{eq}}) \tag{4.14}$$

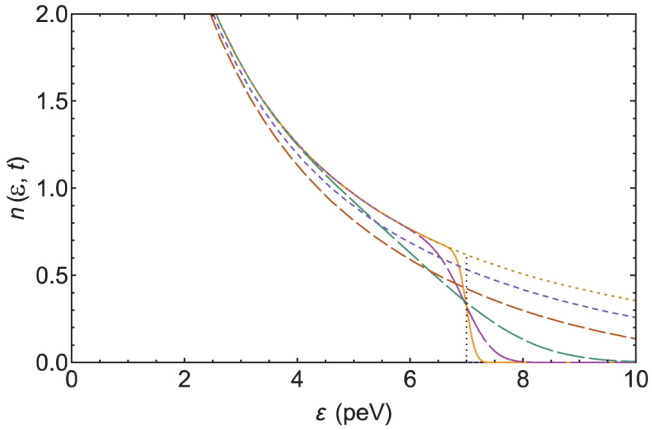

Figure 9: Equilibration of a finite Bose system. Cutoff: 7peV, transport coefficients: $D = 8 \cdot 10^3$ peV^2 s^{-1}, $v = -1 \cdot 10^3$ peV s^{-1}, $T = -D/v = 8$ peV $\simeq 93$ nK, time evolution: $t = 0.001, 0.01, 0.1, 1, 4, 40$ ms (decreasing dash length) [16].

with the initial nonequilibrium distribution $n_i(\epsilon)$, the final equilibrium distribution $n_{eq}(\epsilon)$, and the equilibration time τ_{eq}. Figure 10 shows an evaporative cooling process towards an equilibrium distribution with regard to the linear relaxation ansatz. However, it becomes clear that due to the linear ansatz, the solutions do not lead to a physically correct result. This can be seen as the distribution functions at the cutoff at $\epsilon_i = 7$peV remain discontinuous. In addition, the exponential tail in the UV region $\epsilon > \epsilon_i$ builds up very quickly, not only for large times at which $t \to \infty$, but also for very short times.

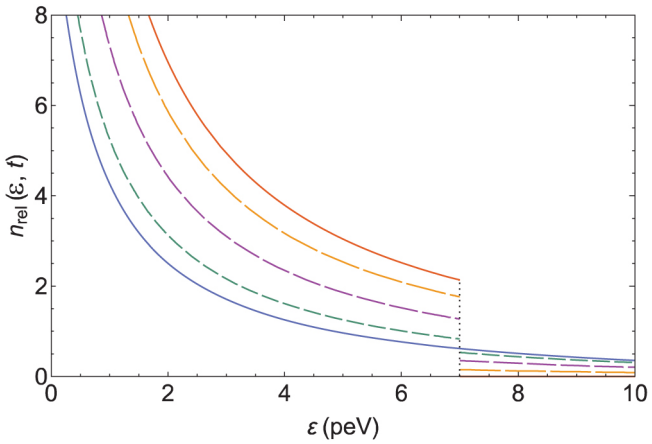

Figure 10: Evaporative cooling in a bosonic system from temperature $T_i = 20$ peV $\simeq$ 232 nK (upper solid curve) to final temperature $T_f = 8$ peV $\simeq 93$ nK (lower solid curve), time evolution: $t = 1, 3, 7$ ms (decreasing dash length) [16].

For these reasons, it is preferable to use the NBDE, which can be used to achieve a significantly more physically correct result compared to the linear relaxation ansatz. Figure

11 shows an evaporative cooling process towards an equilibrium distribution with regard to the NBDE. Evidently, in this situation the time-dependent analytical distribution functions are continuous. In addition, no rapid build-up of the exponential tail occurs in the UV region at short times, but only a very slow build-up due to diffusion.

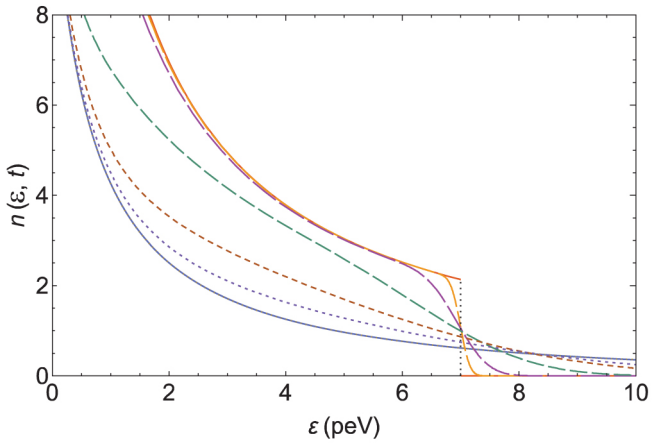

Figure 11: Evaporative cooling in a bosonic system from temperature $T_i \simeq 232$ nK (upper solid curve) to final temperature $T_f = 93$ nK (lower solid curve), time evolution: $t = 0.001, 0.01, 0.1, 0.4, 0.8$ ms (decreasing dash length) [16].

4.3 Time-dependent entropy

One condition that is placed on the solutions of the NBDE is that the entropy increases with time towards the equilibrium value. In the case of a constant temperature, this can be seen very clearly from the monotonous increase in entropy during the time evolution (see Figure 9).
However, in Figures 10 and 11, which include an evaporative cooling process, it can be seen that the entropy decreases due to cooling, but increases again due to thermalization.
The cutoff removes atoms with high energies, which instantly reduces the entropy to about 1/4 of the value compared to the entropy of the equilibrium curve at high temperatures.
The entropy in a Bose system can be expressed by:

$$S(t) = \int_0^\infty g(\epsilon)\Big[\ln\left(1 + n(\epsilon,t)\right) + n(\epsilon,t)\ln\left(1 + 1/n(\epsilon,t)\right)\Big]d\epsilon \tag{4.15}$$

with the average number of particles $n(\epsilon, t)$ per single-particle state. For the density of states $g(\epsilon)$ the following power-law applies:

$$g(\epsilon) = g_0\sqrt{\epsilon} \tag{4.16}$$

with $g_0 = (2m)^{3/2}V/(4\pi^2)$ where $\hbar = c = k_B = 1$. The first term in equation (4.15) is called the *wave entropy*, which particularly plays a role for large occupation numbers. The second term used in equation (4.15) is called the *particle entropy* and is most relevant for low occupation numbers.
Figure 12 shows the time evolution of the entropy $S(t)/g_0$ for the analytical solutions of the NBDE (solid). The equilibrium value of the entropy at initial temperature T_i is $S_{eq}/g_0\ (T_i) \simeq 256.35$ peV$^{3/2}$. With the cutoff at $\epsilon_i = 7$peV the entropy of the initial nonequilibrium distribution is given by $S_i/g_0\ (T_i) \simeq 30.96$ peV$^{3/2}$.
The dashed curve represents the wave entropy. Since large occupation numbers are relevant at all times in the IR region $\epsilon < \epsilon_i$, the curve hardly depends on the time and is therefore largely flat. The yellow-dotted curve represents the particle entropy, which begins slightly below the curve of the wave entropy, because the occupation numbers in the UV energy region are negligible at low times. However, the curve continues to rise due to thermalization, and oversteps the curve of the wave entropy. The violet dotted curve represents the result of the linear relaxation ansatz, which exhibits a steep increase at short times due to the rapid build-up of the exponential tail in the UV energy region. Both the curve of the linear relaxation ansatz and the curve of the nonlinear ansatz aim for the same new equilibrium value at $S_{eq}/g_0\ (T_f) \simeq 61.66$ peV$^{3/2}$, which is represented by the horizontal dotted line.

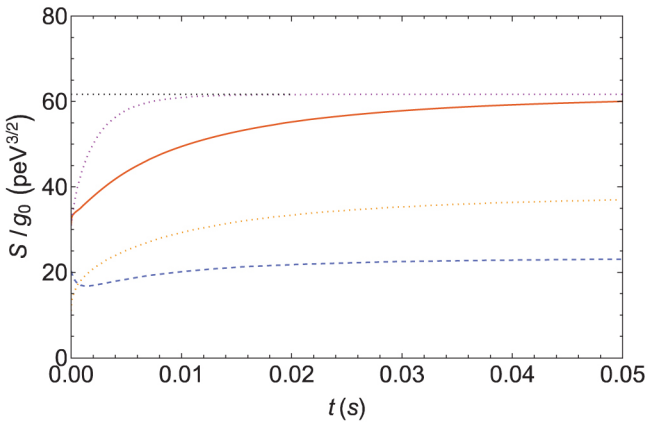

Figure 12: Time evolution of the entropy $S(t)/g_0$ in an equilibrating bosonic system with regard to evaporative cooling from $T_i = 232$ nK to $T_f = 93$ nK [16].

5 Summary and outlook

The properties and use of evaporative cooling were demonstrated in the introductary chapter. Since evaporative cooling provides the possibility to obtain very low temperatures and an increase in the phase space density, it can be used for the generation of Bose-Einstein condensates.
The second chapter presented the model of the Amsterdam group, which indicates that the energy density can be approximated by a truncated Boltzmann distribution. In addition, the application example of the group shows that evaporative cooling in magnetically trapped atomic hydrogen can be used to produce Bose-Einstein condensates.
The third chapter introduced the model of the MIT group, which discussed evaporative cooling using alkali atoms. It has been shown that the Amsterdam model can be applied to this situation to discuss the efficiency of evaporative cooling.
The final chapter presented the results of the Heidelberg group, which discussed exact analytical solutions of an NBDE with regard to the evaporative cooling process, and demonstrated why the inclusion of a singularity is important to achieve physically valuable results, that is, to obtain a thermal equilibrium distribution both in the UV region and the IR region. These results were then used to calculate the time-dependent entropy, whereby the cooling process was seen to lead to a decrease in entropy. However, subsequent thermalization led to an increase in entropy.
The chemical potential has thus far been regarded as a fixed parameter that leads to the violation of particle number conservation. Therefore, it would be helpful to plot the rate of increase of atoms in the condensate $N_c(t)$ in the course of particle number conservation. However, this would imply that the analytical solutions of the NBDE are only approximately valid, since the conservation of the particle number requires a time-dependent chemical potential. [16]
It was recently determined that it is possible to determine the condensate fraction as a function of time without an explicit treatment of the quantum physics of the condensate. The result can be seen in figure 13.

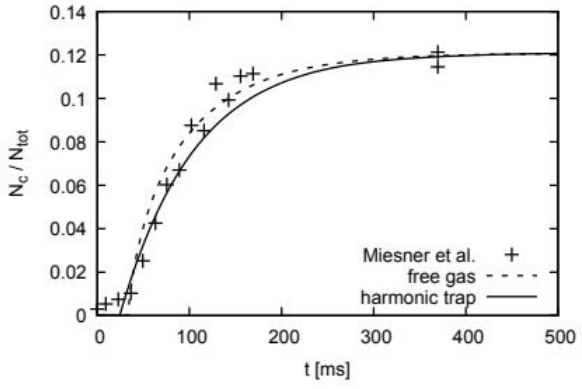

Figure 13: Comparison with data using different density of states , data from Miesner et al., Science, 279, 1005 (1998).

6 Appendix

6.1 Scaling behavior

SCALING LAWS FOR EVAPORATIVE COOLING IN A d-DIMENSIONAL POTENTIAL $U(r) \propto r^{d/\delta}$

Quantity	Exponent , x
Number of atoms, N	1
Temperature, T	α
Volume, V	$\delta\alpha$
Density, n	$1 - \delta\alpha$
Phase-space density, D	$1 - \alpha(\delta + 3/2)$
Elastic collision rate, $n\sigma v$	$1 - \alpha(\delta - 1/2)$

Figure 14: Each quantity scales as N^x [10].

6.2 Incomplete gamma function

Appendix 6.2 was taken from [11] p.41.
The incomplete gamma function is defined by:

$$P(a,\eta) \equiv \frac{1}{\Gamma(a)} \int_0^\eta dt\ t^{a-1} e^{-t} \tag{6.1}$$

with the Euler gamma function $\Gamma(a)$. $P(a,\eta)$ can be expressed as a series expansion:

$$P(a,\eta) = e^{-\eta}\ \eta^a \sum_{m=0}^{\infty} \frac{\eta^m}{\Gamma(m+a+1)} \tag{6.2}$$

which reduces for integer $a = 1, 2, 3, ...$ to

$$P(a,\eta) = 1 - e^{-\eta} \sum_{m=0}^{a-1} \frac{\eta^m}{m!}\ . \tag{6.3}$$

Expansion in terms of $1/\eta$:

$$P(a,\eta) = 1 - e^{-\eta} \frac{\eta^{a-1}}{\Gamma(a)} \Big[1 + \frac{(a-1)}{\eta} + \frac{(a-1)(a-2)}{\eta^2} + ...\Big]\ . \tag{6.4}$$

The derivative of $P(a,\eta)$ with respect to η is given by:

$$\frac{\partial P(a,\eta)}{\partial \eta} = \frac{a}{\eta}[P(a,\eta) - P(a+1,\eta)] = \frac{e^{-\eta}\eta^{a-1}}{\Gamma(a)}\ . \tag{6.5}$$

References

[1] Abramowitz M. and Stegun I.A., Handbook of Mathematical Functions, (Dover, New York 1965)

[2] Walraven J.T.M and Silvera I.F., Phys. Rev. **44**, 168 (1980)

[3] Hess H., Bull. Am. Phys. Soc. [2] **30**, 854 (1985)

[4] Hess H.F., Phys. Rev. B **34**, 3476 (1986)

[5] Luiten O.J., Werij H.G.C., Setija I.D., Reynolds M.W., Hijmans T.W., Walraven J.T.M., Phys. Rev. Lett. **70**, 544 (1993)

[6] Davis K.B., Mewes M.-O., Ketterle W., Appl. Phys. B **60**, 155 (1995)

[7] Davis K.B. , Mewes M.O., Joffe M.A., Andrews M.R., Ketterle W., Phys. Rev. Lett. **74**, 5202 (1995)

[8] Anderson M. H., Ensher J. R., Matthews M. R., Wieman C. E., Cornell E. A., Science **269**, 198 (1995)

[9] Luiten O. J., Reynolds M. W., Walraven J. T. M., Phys. Rev. A **53**, 381−389 (1996)

[10] Ketterle W., van Druten N.J., edited by B. Bederson , H. Walther, Vol. **37**, 181−236 (1996)

[11] Walraven J.T.M., Lecture notes (ch. 3, p. 25−42); published in: Quantum dynamics of simple structures , L. Oppo , S.M. Barnett, E. Riis, M. Wilkinson (Eds.), IOP, Bristol, Vol. **44**, 315−325 (1996)

[12] Surkov E. L, Walraven J.T. M., Shlyapnikov G.V., Phys. Rev. A **52**, xxx (1996)

[13] Wolschin G., Physica A **499**, 1 (2018)

[14] Wolschin G., EPL **123**, 20009, (2018)

[15] Rasch N., Wolschin G., Physics Open **2**, 100013 (2020)

[16] Wolschin G., EPL **129**, 40006 (2020)